Heidi Isabel Villafán Vidales*, Antonio Jiménez-González, Alejandro Bautista-Orozco, Camilo A. Arancibia-Bulnes and Claudio A. Estrada

Solar production of WO_3: a green approach

Abstract: The tungsten trioxide (WO_3) is a promising material with important technologic and scientific applications, due to its electrochromic, gasochromic and photochromic properties. Usually, this material is synthesized following several routes, for example, sputtering, chemical deposition, sol-gel, hydrothermal, among others. However, these methods are complicated, have long processing times and use several chemicals with the possibility of keeping undesirable impurities. In this context, concentrated solar energy is an interesting and feasible option to process materials at a low cost and without greenhouse gas emissions. In this work, a simple and green synthesis method of WO_3 by using the Solar Furnace of the Renewable Energy Institute of the National University of Mexico is presented. Tungsten oxide powder is obtained by means of tungsten electrodes in a high-temperature solar reaction chamber designed to work with concentrated solar energy under controlled conditions of the gas atmosphere. The oxidation reaction was carried out for three different temperatures: 600°C, 800°C and 1000°C, and for each temperature three different oxygen molar fractions were studied: 0.33, 0.41 and 1. Some results indicate the oxygen molar fraction does not affect the phase transformation and the WO_3 triclinic was the most stable phase, appearing in all the temperature ranges and concentrations. The synthesis reported in this paper is presented as a green alternative in the development of processes for the synthesis of WO_3, which promote renewable energy sources with very low greenhouse gas emissions and without toxic residuals.

Keywords: concentrated solar energy; green WO_3 synthesis; solar chemistry; solar furnace; WO_3 synthesis.

DOI 10.1515/gps-2014-0102
Received December 16, 2014; accepted March 18, 2015; previously published online April 25, 2015

***Corresponding author: Heidi Isabel Villafán Vidales,** Instituto de Energías Renovables, Universidad Nacional Autónoma de México, Privada Xochicalco S/N, 62580 Temixco, Mexico,
e-mail: hivv@ier.unam.mx
Antonio Jiménez-González, Alejandro Bautista-Orozco, Camilo A. Arancibia-Bulnes and Claudio A. Estrada: Instituto de Energías Renovables, Universidad Nacional Autónoma de México, Privada Xochicalco S/N, 62580 Temixco, Mexico

1 Introduction

Tungsten trioxide (WO_3) has been the focus of several research works due to its optical, chemical, photochromic, gasochromic and electrochromic properties. For example, it has been used in the photocatalysis area because it possesses a wide band gap energy that ranges from 2.4 to 2.8 eV [1]. It also has been also used as chemical sensor or inclusive in optic applications [2, 3].

This material has been synthesized by numerous liquid-phase synthesis routes, including sol-gel, hydrothermal and electrochemical anodization. The main disadvantages of these methods are that they involve several intermediate steps, have long processing times (depending on the method) and use several chemicals with the possibility of keeping undesirable impurities. For example, in the sol-gel method, some acids are taken as precursors for the WO_3 synthesis [4]. The hydrothermal synthesis needs also some chemical precursors, sometimes sulfates or nitrates at relative medium temperatures (ranging from 120°C to 300°C), which usually are provided with electricity from fossil fuels. Conversely these methods possess some advantages, such as low cost and easy control of the particle size and the shape crystalline structure of the tungsten oxide.

By contrast, concentrated solar systems can be used to provide the heat of the reaction at very high temperatures. For example in the solar furnace of the Renewable Energy Institute of UNAM in Mexico (HoSIER by its acronym in Spanish) it is possible to reach temperatures as high as 3400°C in a few seconds. This particular feature of solar furnaces projects them as a potential tool for the materials processing. Some examples of the synthesis of materials with concentrated solar energy are: synthesis of fullerenes [5–9]; synthesis of tungsten carbide [10–12]; synthesis of molybdenum carbide [13]; synthesis of calcium carbide [14]; and processing of silicon carbide [15–18]. The main disadvantages of solar processes are the intermittent nature of solar energy and the initial investment costs of solar systems.

In this paper concentrated solar energy was used to synthesize WO_3 at high temperatures. This route to produce tungsten oxides has not been previously reported. The WO_3 synthesis reported in this work is presented as a green alternative in the development of processes for

the synthesis of WO_3, which promote renewable energy sources with very low greenhouse gas emissions and without toxic residuals.

The WO_3 solar synthesis was carried out in a reaction chamber designed to work under controlled atmospheres. The reaction was carried out for three different temperatures: 600°C, 800°C and 1000°C, and for each temperature three different oxygen molar fractions were studied: 0.33, 0.41 and 1. Some results indicate the oxygen molar fraction does not affect phase transformations and the triclinic structure of WO_3 was the most stable phase, found in all the temperature ranges and concentrations.

2 Materials and methods

WO_3 was synthesized at high-temperatures provided by the HoSIER [19]. The HoSIER consists of a flat-heliostat (81 m^2 area) and a faceted-concentrator (36 m^2 area) with focal length of 3.68 m and focal zone of 7 cm diameter. At the focal point, the maximal flux density is 18,000 suns (1 sun=1 kW/m^2) with Gaussian distribution [20]. Between the heliostat and the concentrator, there is a shutter that was used to control the temperature in the sample (Figure 1).

For the WO_3 synthesis, commercial electrodes of pure tungsten bars were used as a raw material (Weld 500, 94% purity, USA). These 1.8" diameter electrodes form a flat plate of 17.8 cm length and 2.4 cm height. This tungsten plate was placed at the focal zone of the concentrator and at the center of a reaction chamber designed to work under controlled atmospheres.

The reaction chamber features a Pyrex spherical glass vessel of 25 l capacity, 35 cm diameter and 65 cm height (Figure 2).

At the bottom of the reaction chamber, a rotary vacuum pump was connected in order to control the total pressure and to ensure the continuous gas flow inside the reactor. Additionally, several gases were introduced into the chamber: Argon (Ar), oxygen (O_2) or a mixture of Ar with O_2 (Figure 2). The pressure was monitored with a DualTrans vacuum transducer (Mod. 910, 1×10^{-5} to 1500 Torr range, MKS, Boulder, CO., USA), and the temperature on the sample with three type "K" thermocouples placed in three different positions: at the center of the sample (T1=75 mm), at 35 mm from the center (T2) and near the sample holder (T3=0 mm) (Figure 3).

At the beginning of each experiment, the vacuum pump was started with the aim of eliminating the air atmosphere inside the reaction chamber (10^{-2} bar pressure). Subsequently, Ar gas (99.95% purity, Infra, Mexico) was injected into the chamber in order to assure an inert atmosphere inside the chamber (0.5–0.6 bar). Once the pressure was stabilized, the sample was gradually heated with concentrated solar energy until it reached the desired temperature (600°C, 800°C or 1000°C). In this case, the heated area was 17 cm^2. Then, O_2 gas (99.95% purity, Infra, Mexico) was introduced into the chamber in three different molar fractions (0.33, 0.41 and 1) and the total pressure was incremented to 0.8 bar.

During experimentation, the chamber was operated for direct normal irradiation above 800 W/m^2 and total pressures of 0.8 bar. Every experiment had a reaction period of 20–30 min. The progressive formation of a tungsten oxide film and some crystals (depending on the temperature) was observed, especially in the non-directly irradiated zone.

At the end of experimentation, the sample was collected and analyzed by several techniques. The crystalline phase identification of the oxides was performed by the X-ray diffraction technique (XRD) using a CuKα line with a wavelength λ=1.542 Å (Rigaku diffractometer, Mod. DMAX-2200 and Ultima IV, Tokyo, Japan). The surface of the oxidized samples was analyzed by scanning electron microscopy (SEM) and energy dispersive spectroscopy (Hitachi Mod. SU1510, Tokyo, Japan).

3 Results and discussion

The general oxidation reaction of tungsten is the following:

$$2W + 3O_2 \rightarrow 2WO_3 \quad (1)$$

The oxidation of tungsten was carried out at three different temperatures: 600°C, 800°C and 1000°C, and for each

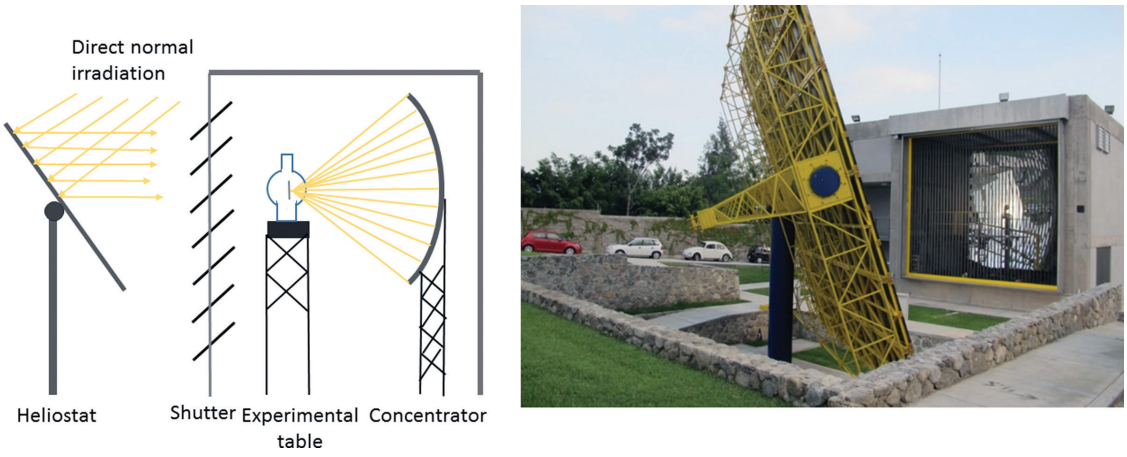

Figure 1: Schematic operation of the Instituto de Energías Renovables of Universidad Nacional Autónoma de México (IER-UNAM) solar furnace.

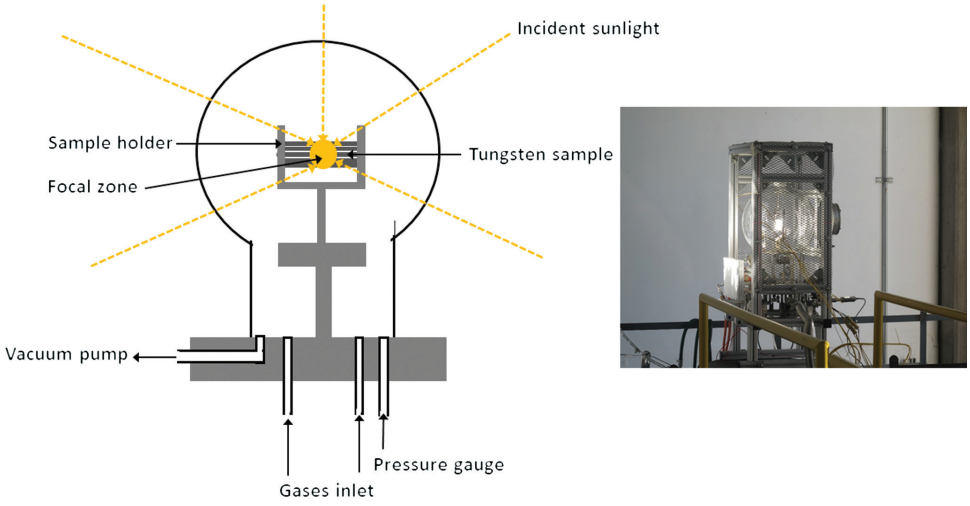

Figure 2: Schematic view of the reaction chamber.

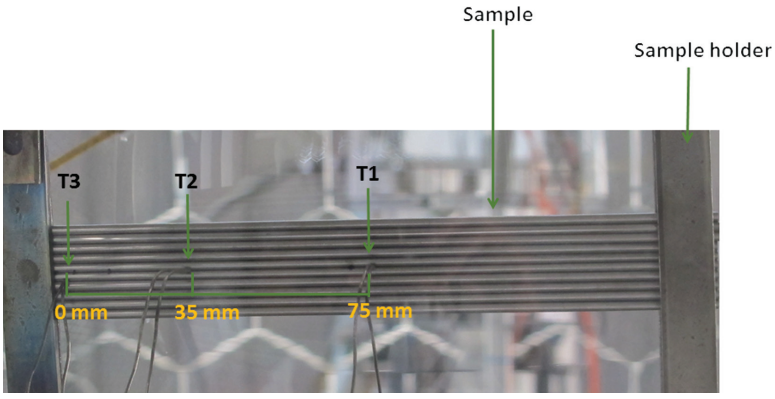

Figure 3: Schematic view (or picture) of tungsten bars with of thermocouples type "K" mounted on three different positions of the sample.

temperature, three different oxygen molar fractions were studied: 0.33, 0.41 and 1.

3.1 Tungsten bars oxidation at 600°C

During tungsten oxidation at 600°C at different oxygen molar fractions (Y_{O_2}), it is possible to observe the formation of a yellow film on the front side of the tungsten bars. This film was formed especially in the directly irradiated zone (high temperature zone), as shown in Figure 4. Around this zone, the formation of a thin blue/black film is visible. The apparition of this blue/black film was previously reported by several authors [21, 22]. Kellet and Rogers [22] found that this film is protective avoiding the diffusion of oxygen through the oxide layer, whereas the yellow film is nonprotective.

For an O_2 molar fraction of 0.33, the yellow powder grows on the tungsten surface forming a thin film (Figure 4A). The film thickness increases incrementing the oxygen content in the chamber (0.41 O_2 molar fraction), as shown in Figure 4B. In this case, the oxygen starts to produce cracks on the tungsten surface. These cracks promote the oxygen transport inside the tungsten, helping the reaction take place inside tungsten bars leading to an increment in the thickness of the film. The cracking mechanism was previously described by Gulbransen and Andrew [23]. According to these authors, the formation of tungsten oxides is a cyclic mechanism. At the beginning of oxidation a thin layer of oxide is formed, then after reaching a certain thickness, the tungsten oxide cracks in local areas. These local areas give access to the remaining oxygen, forming again a layer of certain thickness leading to the formation of deeper cracks and the formation of a thicker film.

In a highly oxidizing atmosphere (Y_{O_2}=1), tungsten rapidly reacts with oxygen, obtaining crystals oriented perpendicularly to the sample (Figure 4C).

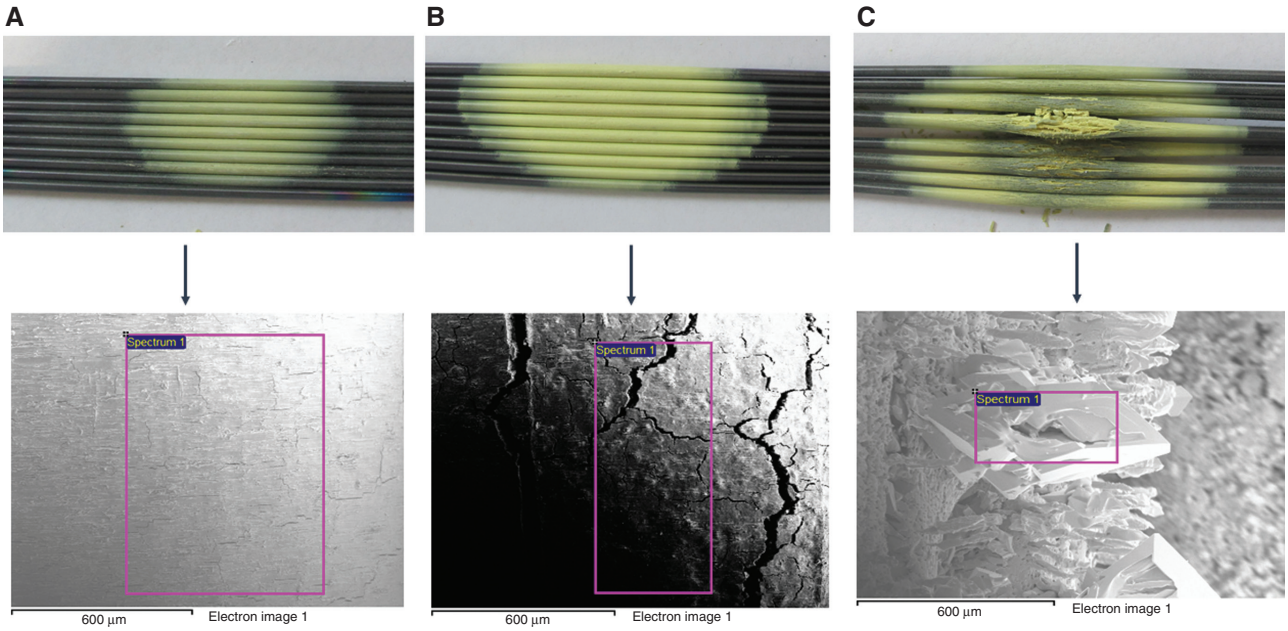

Figure 4: Photographs and scanning electron microscopy (SEM) micrographs of directly irradiated zone of the samples under experimental conditions of temperature (600°C) with O_2 molar fraction of: (A) 0.33, (B) 0.41 and (C) 1.

The XRD analyses of the yellow zone of the three samples demonstrate that the yellow powder corresponds to WO_3 with triclinic cell parameters of a=7.3 Å, b=7.52 Å and c=7.69 Å; and orthorhombic phases with cell parameters of a=7.38 Å, b=7.51 Å and c=3.84 Å. For the blue/black zone, it was found that this compound corresponds to $W_{24}O_{68}$ ($WO_{2.83}$) with cell parameters of a=19.3 Å, b=3.78 Å and c=17.07 Å, but a strong diffraction pattern of tungsten from the underlying layer was also found (Figure 5).

This effect was previously observed by Kellet and Rogers [22]. They affirm that the film of a nonstoichiometric tungsten oxide has a few microns due to the presence of the strong diffraction pattern of W in the XRD analysis. In this case, the same effect is corroborated with the diffraction pattern.

In this set of experiments, the WO_3 particles had an average particle size of 38 nm.

3.2 Tungsten bars oxidation at 800°C

The following experiments were carried out at 800°C. During this set of experiments, it was found that some of the formed tungsten oxide sublimes. This phenomena was previously observed in the same temperature range by Gulbransen and Andrew [23] and Baur et al. [24]. During experimentation some of the volatilized tungsten oxide was deposited on the reactor walls forming a yellowish thin film. For all cases, the recollected powder corresponds to WO_3 with monoclinic (cell parameters: a=7.3 Å, b=7.53 Å and c=7.68 Å) and epsilon-monoclinic phases with cell parameters of a=5.27 Å, b=5.16 Å and c=7.67 Å (Figure 6).

At this temperature, tungsten has a poor resistance to oxidation. When the atmosphere has an oxygen molar fraction of 0.33, the tungsten bars show some deformation followed by several cracks and the formation of some crystals in the form of needles oriented perpendicularly to the tungsten surface (Figure 7A).

For an oxygen molar fraction of 0.41, the front side of the tungsten bars also suffers some deformation. In this case, the center of the front surface (directly irradiated zone) begins to reduce it size and does not exhibit porosity (gray zone, Figure 7B1). Around this zone, the formation of some crystals and cracks is observed. By contrast, SEM micrographs on the rear part of this sample revealed the formation of many crystals with a very particular form (Figure 7B2).

In a highly oxidant atmosphere (Y_{O_2}=1), the tungsten bars also suffer deformation, but in this case, the sample exhibits a perforation in the high temperature zone. Below the perforation, it is possible to observe the formation of some melt. SEM micrographs of the yellow zone around the perforation revealed the formation of some crystals in the form of crosses (Figure 7C).

The XRD analyses in the formed crystals (rear and front side) and yellow layers of all the samples show

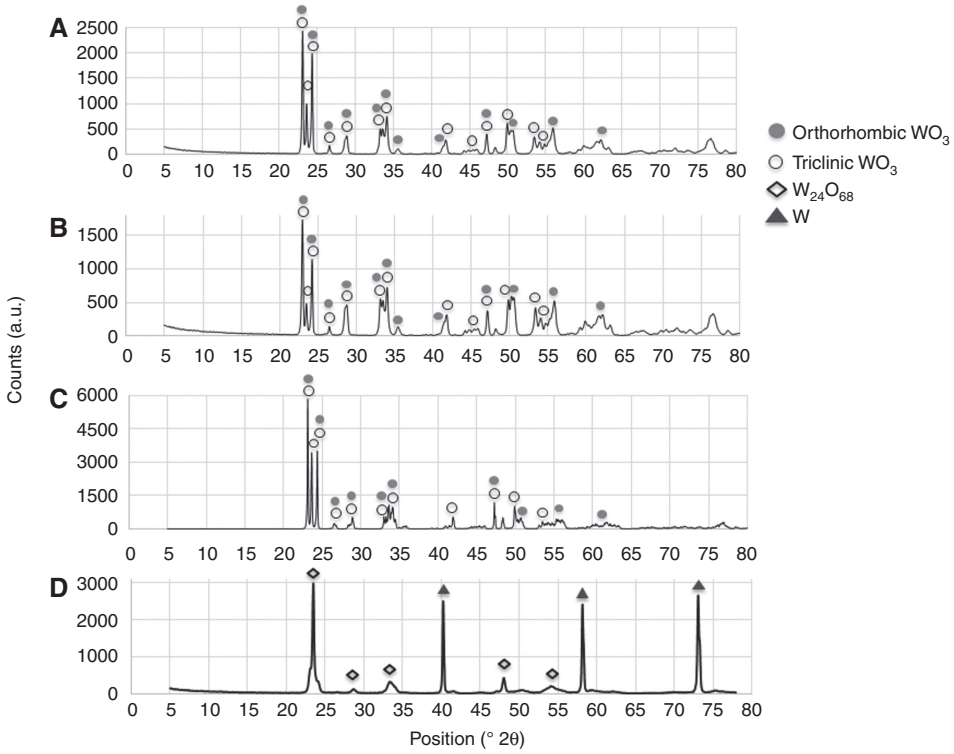

Figure 5: Diffraction patterns of the yellow film under experimental conditions: temperature of 600°C and O_2 molar fraction of: (A) 0.33, (B) 0.41, (C) 1 and (D) blue/black zone.

that this material is WO_3 with two different crystal structures, monoclinic and triclinic. The melt corresponds to monoclinic (cell parameters: a=7.3 Å, b=7.53 Å and c=7.68 Å) and triclinic WO_3 with cell parameters of a=7.31 Å, b=7.52 Å, and c=7.689 Å (Figure 8). At this temperature, the WO_3 particles exhibit an average particle size of 84 nm.

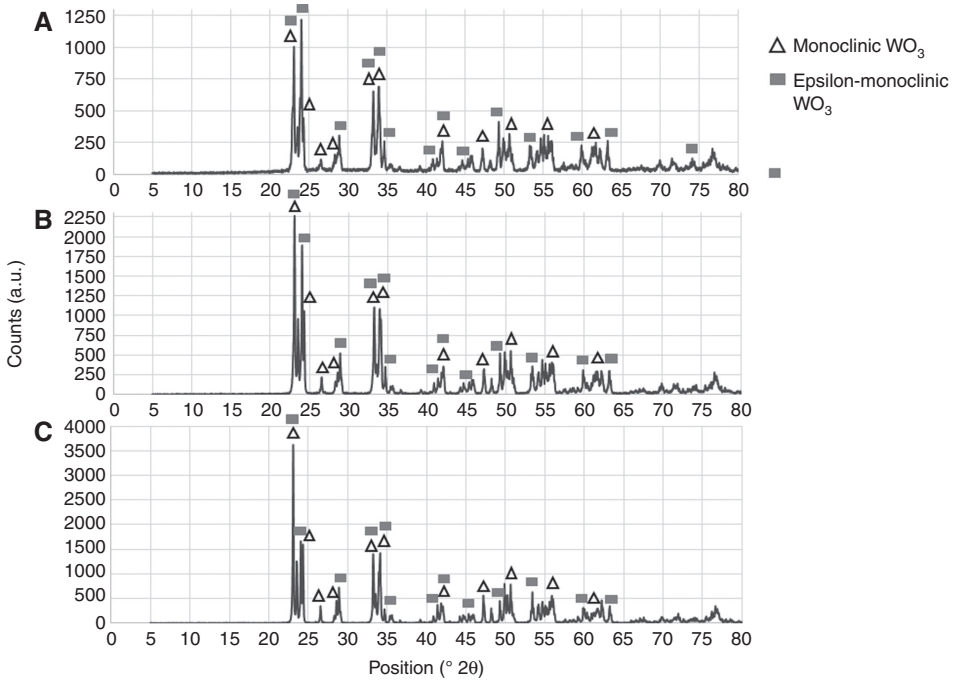

Figure 6: Diffraction patterns of the yellowish thin film deposited on the reaction chamber walls under experimental conditions: temperature of 800°C and O_2 molar fraction of: (A) 0.33, (B) 0.41 and (C) 1.

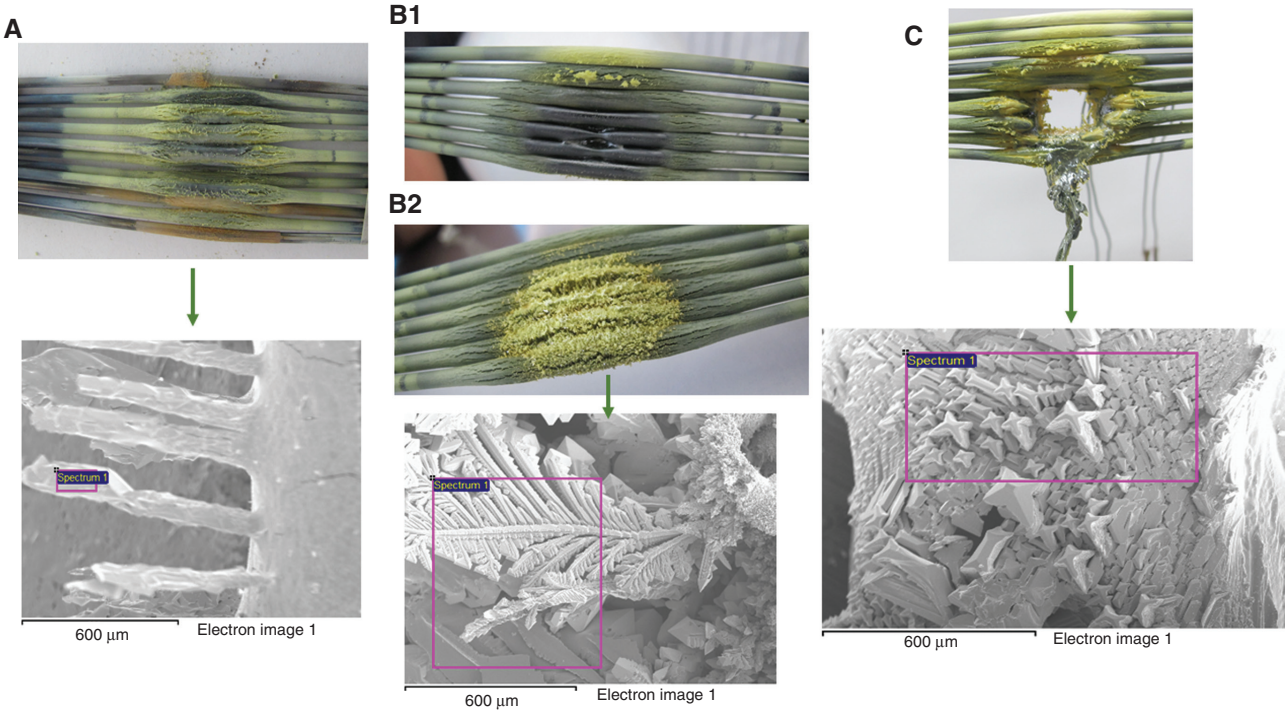

Figure 7: Photograph and scanning electron microscopy (SEM) micrographs of the samples under experimental conditions of temperature (800°C) and O_2 molar fraction of (A) 0.33; (B1, B2) 0.41; (C) 1. (B1) Directly irradiated zone; (B2) Non-directly irradiated zone.

The reduction of the bars in the directly irradiated zone and formation of some cracks and crystals around it (0.41 oxygen molar fraction, Figure 7B) might be due to the temperature gradients obtained during experimentation. Experimentally, measured temperatures in the three different zones of the rear part of the sample are shown in Figure 9. It is observed that in a short distance there is a maximal temperature difference of 190°C between the center (T1) and 35 mm apart from the center (T2) of the sample. In the center of the rear part of the sample, the temperature is around 800°C, but in the directly irradiated zone (front of the sample), the temperature is higher. The high temperature reached in the front of the sample causes the rapid oxidation of W and sublimation of the formed WO_3 avoiding the formation of a WO_3 film, whereas in the rear part, the reached temperatures promote the formation of several crystals. At 35 mm apart from the center of the sample, the temperature is in the range of 600–720°C (T2, Figure 9). These temperatures promote the formation of cracks and some crystals. Near the sample holder, the temperature is below 550°C (T3, Figure 9). In this zone, the oxygen forms a protective blue/black film, similarly to the low temperature experiments (T=600°C).

WO_3 has a melting point of 1474°C [25], therefore the presence of WO_3 melt might indicate that the center and front of the sample reached at least this temperature. It must be noted that the temperature measurement by type "K" thermocouples was made in the back side of the sample (non-directly irradiated zone) because temperature measurement from the front surface was difficult, due to the presence of radiative concentrated flux, unless a solar-blind IR camera is used in order to eliminate the contribution of the reflected radiation in the temperature measurements. By contrast, the sublimation of WO_3 begins at 750°C and becomes substantial at 900°C [26]. In this experiment, part of the formed WO_3 sublimates due to high temperatures (800°C) and condensates in the chamber walls, as mentioned above.

3.3 Tungsten bars oxidation at 1000°C

The last set of experiments was carried out at a temperature of 1000°C with the same oxygen molar fractions (Y_{O_2} =0.33, 0.41 and 1). As in the above case, some of the formed tungsten oxide sublimates while XRD analyses reveal that this oxide is WO_3 with monoclinic (cell parameters of a=7.3 Å, b=7.53 Å and c=7.689 Å) and epsilon-monoclinic crystalline structures, with cell parameters of a=5.27 Å, b=5.16 Å, and c=7.67 Å.

In all cases, the high temperature combined with an oxidant atmosphere produces some melt, which is below the high temperature zone (Figure 10A1, 10B1 and 10C1). As

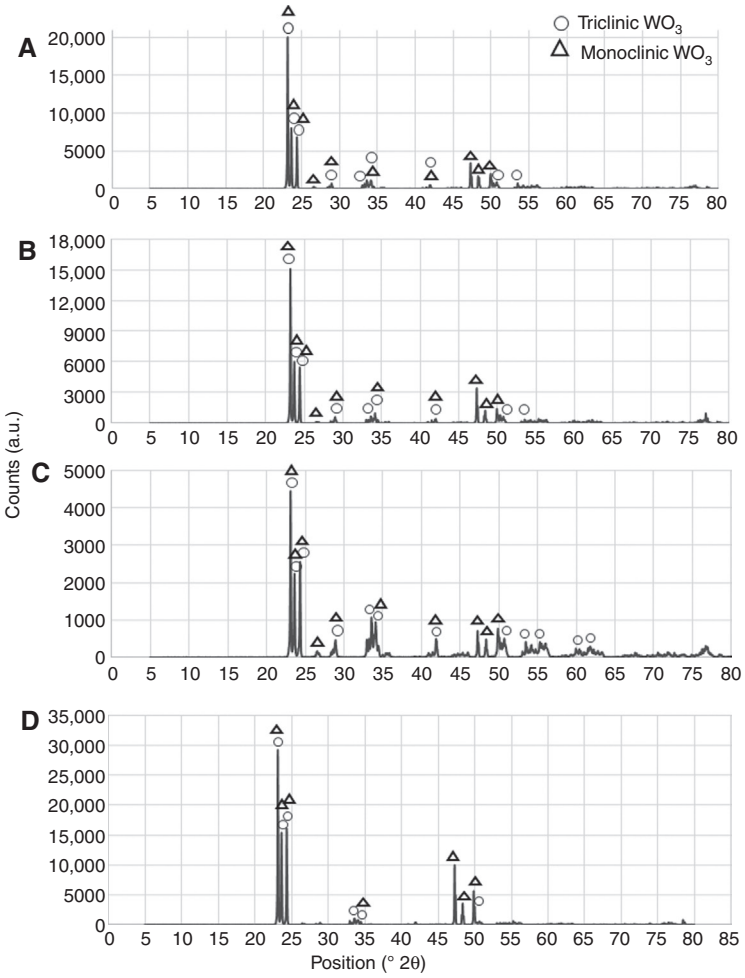

Figure 8: Diffraction patterns of sample the under experimental conditions: temperature of 800 °C, O_2 molar fraction of (A) 0.33, yellow layer; (B) 0.41, crystals; (C) 1, crystals and (D) 1, melt.

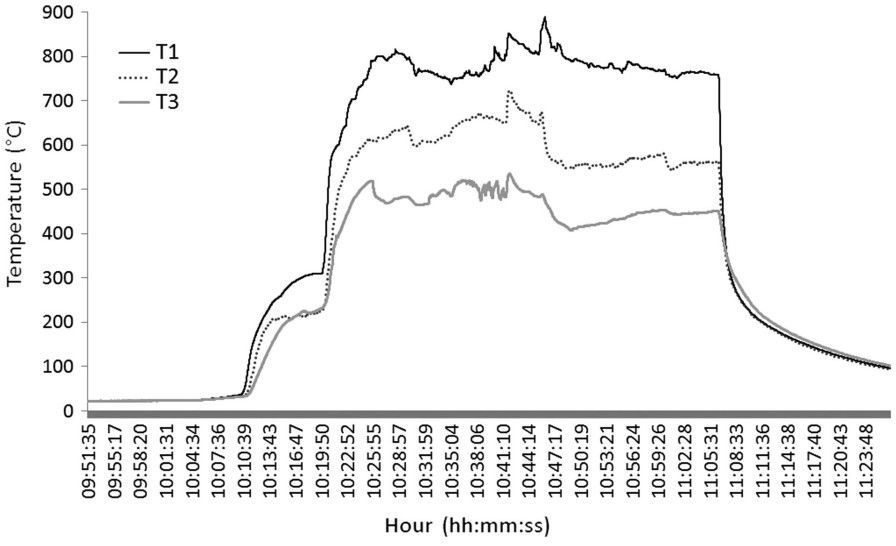

Figure 9: Temperature as a function of time in the three zones of rear part of the sample. T1, center of the sample; T2, 35 mm apart from the center and T3, near the sample holder (75 mm apart from the center).

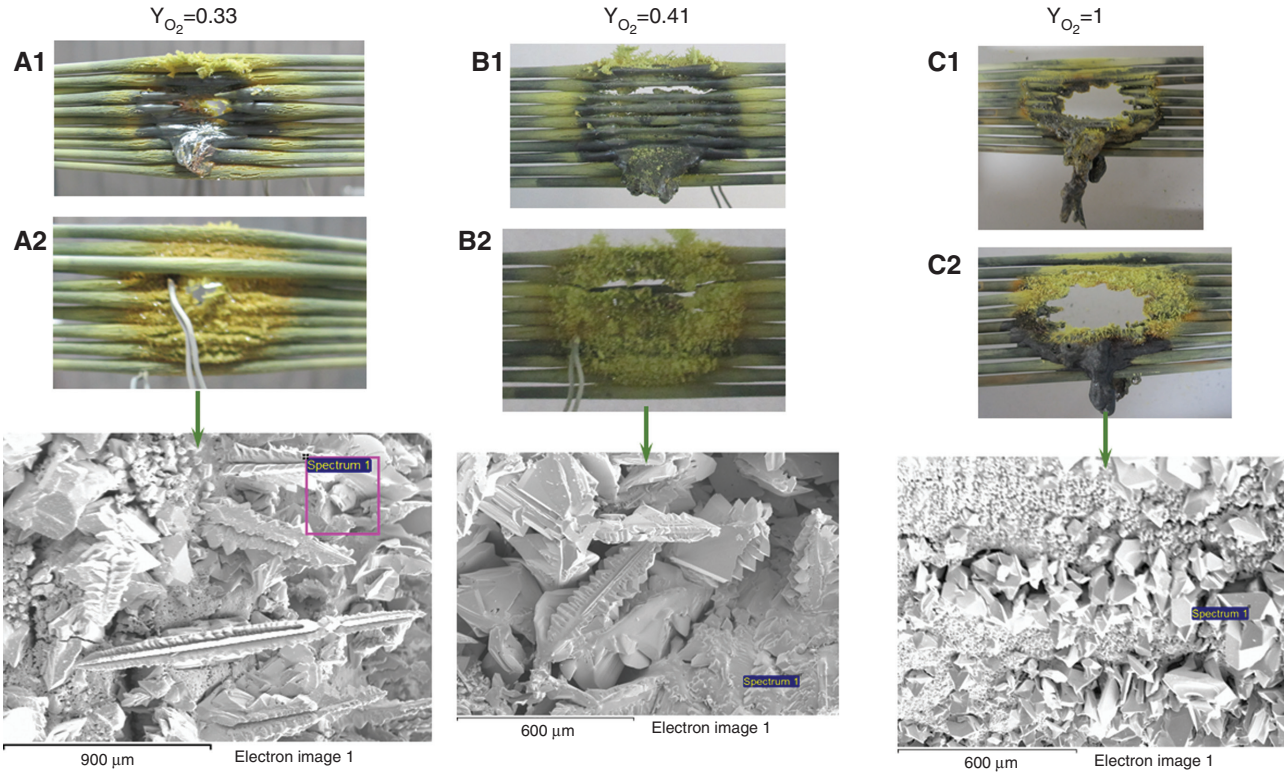

Figure 10: Photograph and scanning electron microscopy (SEM) micrographs of samples after experimentation at 1000°C. Oxygen molar fraction of 0.33: (A1) directly irradiated zone, (A2) non-directly irradiated zone; O_2 molar fraction of 0.41: (B1) directly irradiated zone, (B2) non-directly irradiated zone; O_2 molar fraction of 1: (C1) directly irradiated zone, (C2) non-directly irradiated zone.

mentioned above, this melt might indicate that the front of the sample (directly irradiated zone) reached 1474°C.

In the non-irradiated zone (rear part of the sample), the formation of several crystals is observed (Figure 10A2, 10B2 and 10C3). SEM micrographs in the crystals reveal a particular structure similar to a "pine", except for a highly oxidant atmosphere (Y_{O_2}=1) where the structure is not well defined.

For an O_2 molar fraction of 0.33, the sample presents a small hole in the center of the sample (directly irradiated zone), but in the rear part of the sample is observed the formation of several crystals, like in experiments at 800°C temperature. By contrast, when increasing the oxygen molar fraction (Y_{O_2}=0.41), the bars only decrease in thickness, especially in the directly irradiated zone, whereas in the rear part of the sample the reached temperatures promote the formation of crystal structures. For an O_2 molar fraction of 1, the hole increases its size and the formation of melt appears on both sides of the sample (directly and non-directly irradiated zones).

XRD analyses in the melt and crystals show that WO_3 with triclinic (cell parameters of a=7.31 Å, b=7.525 Å and c=7.689 Å) and a mixture of triclinic and monoclinic (cell parameters of a=7.3 Å, b=7.53 Å and c=7.68 Å) crystalline structures are formed for the three different oxygen molar fractions, respectively. In this case, the WO_3 particles had an average particle size of 104 nm.

The Brunauer-Emmett-Teller (BET) surface area analysis on different samples showed that the superficial area of the samples is small, <1 m^2/g and also that, the volume of the pore is quite small, $<1\times10^{-4}$ cc/g. The pore diameter is also quite small, around 1 Å. Based on the above results, the WO_3 powder is nonporous.

A summary of the XRD analyses at several experimental conditions is depicted in Table 1. During experimentation with different oxygen molar flow concentrations, it was found that the temperature slightly affects the WO_3 phase. The WO_3 orthorhombic phase was only found in the low temperature experiments.

By contrast, the oxygen molar fraction does not affect the phase transformation. The WO_3 triclinic was the most stable phase, appearing in all the temperature ranges and concentrations.

The WO_3 phase on the melt and the deposit on the chamber walls are not affected by the temperature, neither the oxygen concentration.

These results showed that it is possible to use concentrated solar energy for the synthesis of WO_3, mainly with

Table 1: Summary of the different experimental conditions and X-ray diffraction technique (XRD) results.

Temperature (°C)	O_2 molar fraction	Zone	Phase
600	0.33, 0.41, 1	Yellow film (directly irradiated zone)	WO_3 triclinic, orthorhombic
600	0.33, 0.41, 1	Blue/black film (around directly irradiated zone)	$W_{24}O_{68}$
800	0.33, 0.41, 1	Deposit on the chamber walls	WO_3 monoclinic, epsilon-monoclinic phases
800	0.33	Crystals and yellow layers	WO_3 monoclinic, triclinic
800	1	Melt	WO_3 triclinic
1000	0.33, 0.41, 1	Deposit on the chamber walls	WO_3 monoclinic, epsilon-monoclinic
1000	0.33, 0.41, 1	Crystals	WO_3 triclinic, monoclinic phases
1000	0.33, 0.41, 1	Melt (directly irradiated zone)	WO_3 triclinic
1000	1	Melt (non-directly irradiated zone)	WO_3 triclinic

triclinic and monoclinic crystalline structures, by a simple method with lower CO_2 emissions than conventional methods and without the formation of toxic residuals.

However, the reaction only occurs in the center of the sample (directly irradiated zone) and a noticeable amount of unreacted W remained in the samples at the end of the process. This can be avoided by optimizing the operating conditions, for example, using a solar reactor designed specifically to carry out this kind of process, which should allow a more uniform heating of the entire sample. This is a requirement to increase reaction extent.

4 Conclusions

WO_3 has been thermally prepared with success, using concentrated solar energy provided by the Instituto de Energías Renovables of Universidad Nacional Autónoma de México (IER-UNAM) solar furnace (HoSIER) and through a green synthesis method due to a low CO_2 emission process, and avoiding the presence of toxic residuals impurities.

The following conclusions were obtained from the synthesis work. In all of the experiments, it a blue/black film was found that corresponds to a nonstoichiometric tungsten oxide, $W_{24}O_{68}$. This film was obtained in the low temperature zone (near the sample holder) where the sample reaches a temperature of 500°C.

In the low temperature experiments (600°C), it was found that the oxidation reaction of tungsten appreciably improves, especially when the oxygen concentration is increased leading to the formation of cracks on the tungsten surface.

At a temperature of 800°C, the formation of several WO_3 crystals with particular shapes, like needles, ferns and crosses was observed. In a highly oxidant atmosphere, the formation of some melt was also observed, which might indicate that the front of the sample reached at least 1474°C.

In the high temperature experiments (1000°C), the melting point of tungsten oxide was also reached in the front of the sample, indicating that the front of the sample reached at least 1474°C.

Finally, it was found that the temperature slightly affects the WO_3 crystalline phase. By contrast, at a constant temperature, the oxygen molar fraction does not affect the crystalline phase transformation of WO_3. The triclinic WO_3 was the most stable phase, appearing in all the temperature ranges and concentrations. The WO_3 particle size increases when increasing temperature. The BET analysis on the WO_3 powder indicated that this material is nonporous.

In all experiments, some of the metallic tungsten remains unreacted. This can be avoided by optimizing the operating conditions, for example, using a solar reactor designed specifically to carry out this kind of processes, which should allow a more uniform heating of the entire sample leading to a more efficient process.

Acknowledgments: This work was supported by CONACyT (Mexico) through grant 123767. The authors thank R. Rubí-Delgado and R. Morán-Elvira (IER-UNAM) for the reaction chamber design and the technical assistance to J.J. Quiñones-Aguilar (IER-UNAM). The authors would also like to thank M.L. Ramón García and P. Altuzar-Coello (IER-UNAM) for helping with the XRD analysis, and J. Campos-Álvarez (IER-UNAM) for the SEM images.

References

[1] Guo Y, Quan X, Lu N, Zhao H, Chen S. *Environ. Sci. Technol.* 2007, 41, 4422–4427.
[2] Ashraf S, Blackman CS, Palgrave RG, Parkin IP. *J. Mater. Chem.* 2007, 17, 1063–1070.
[3] Cantalini C, Atashbar MZ, Li Y, Ghantasala MK, Santucci S, Wlodarski W, Passacantando M. *J. Vac. Sci. Technol. A* 1999, 17, 1873–1879.

[4] Monro R, Krämer S, Zapp P, Krug H. *J. Sol-Gel Sci. Technol.* 1998, 13, 673–678.
[5] Fields CL, Pitts J, Hale MJ, Bingham C, Lewandowski A, King DE. *J. Phys. Chem.* 1993, 97, 8701–8702.
[6] Chibante LPF, Thess A, Alford JM, Diener MD, Smalley RE. *J. Phys. Chem.* 1993, 97, 8696–8700.
[7] Laplaze D, Bernier P, Flamant G, Lebrun M, Brunelle A, Della-Negra S. *J. Phys. B: At. Mol. Opt. Phys.* 1996, 29, 4943–4954.
[8] Laplaze D, Bernier P, Flamant G, Lebrun M, Brunelle A, Della-Negra S. *Synth. Met.* 1996, 77, 67–71.
[9] Flamant G, Luxembourg D, Rober JF, Laplaze D. *Sol. Energy* 2004, 77, 73–80.
[10] Shohoji N, Guera Rosa L, Cruz Fernandes J, Martínez D, Rodríguez J. *Mater. Chem. Phys.* 1999, 58, 172–176.
[11] Almeida Costa Oliveira F, Cruz Fernandes J, Badie JM, Granier B, Guerra Rosa L, Shohoji N. *Int. J. Refract. Met. Hard Mater.* 2007, 25, 101–106.
[12] Almeida Costa Olivera F, Granier B, Badie JM, Cruz Fernandes J, Guerra Rosa L, Shohoji N. *Int. J. Refract. Met. Hard Mater.* 2007, 25, 351–357.
[13] Guerra Rosa L, Cruz Fernandes J, Amaral PM, Martínez D, Rodríguez J, Shohoji N. *Int. J. Refract. Met. Hard Mater.* 1999,17, 351–356.
[14] Paizullakhanov MS, Faiziev ShA. *Tech. Phys. Lett.* 2006, 32, 211–212.
[15] Cruz Fernandes J, Amaral PM, Guerra Rosa L, Martínez D, Rodríguez J, Shohoji N. *Int. J. Refract Met. Hard Mater.* 1999, 17, 437–443.
[16] Cañadas I, Martínez D, Rodríguez J. *Bol. Soc. Esp. Ceram. V.* 2004, 43–2, 591–595.
[17] Gulamova DD, Uskebaev DE, Turdiev ZhSh, Toshmurodov YoK, Bobokulov SH. *Appl. Sol. Energy* 2009, 45, 105–108.
[18] Lu L, Chan BCY, Wang X, Chua HT, Raston CL, Albu-Yaron A, Levy M, Popowitz-Biro R, Tenne R, Feuermann D, Gordon JM. *Nanotechnology* 2013, 24, 335603, 7pp.
[19] Estrada CA, Arancibia CA, Vázquez S, Pérez CA, Riveros D, Pérez R, Quiñones J, Castrejón R, Montiel M, Granados F. *SolarPACES Symposium* 2011, Spain.
[20] Riveros-Rosas D, Herrera-Vázquez J, Pérez-Rábago CA, Arancibia-Bulnes CA, Vázquez-Montiel S, Sánchez-González M, Granados-Agustín F, Jaramillo OA, Estrada CA. *Sol. Energy* 2010, 84, 792–800.
[21] Webb WW, Norton JT, Wagner C. *J. Electrochem. Soc.* 1956, 103, 107–111.
[22] Kellet EA, Rogers SE. *J. Electrochem. Soc.* 1963, 110, 502–504.
[23] Gulbransen EA, Andrew KF. *J. Electrochem. Soc.* 1960, 107, 619–628.
[24] Baur JP, Bridges DW, Fassell MW Jr. *J. Electrochem. Soc.* 1956, 103, 266–272.
[25] Wriedt HA, *Bull. Alloy Phase Diagrams* 1989, 10, 368–384.
[26] Williamson EH, Yao N. *Nanotechnology in Catalysis 3*, Zhou B, Han S, Raja R, Somorjai GA, Eds., Springer: New York, Vol. 3, p 177.

Bionotes

Heidi Isabel Villafán Vidales

Heidi Isabel Villafán Vidales has been an associate researcher at Instituto de Energías Renovables, Universidad Nacional Autónoma de México (IER-UNAM) since 2011. She obtained her PhD in Energy Engineering in 2009 and from 2010–2011, she worked as a post-doctoral research assistant at the Procedes, Materiaux et Energie Solaire Laboratory (France). Her research is focused on solar fuels production, CO_2 recycling and upgrading for synthetic liquid fuel production, solar chemical reactors and solar synthesis.

Antonio Esteban Jiménez González

Antonio Esteban Jiménez González, a physicist from Instituto Politécnico Nacional (IPN, México D.F.), obtained an MSc in physics (IPN, México D.F) and a PhD in physics at the University of Tuebingen, Germany. He has been senior researcher at IER-UNAM since 1992. His main research interests are related to solid state physics, semiconductor physics and surface science, with applications to solar chemical reactors, dye sensitized solar cells and photocatalysis in the aqueous phase.

Alejandro Bautista Orozco

Alejandro Bautista Orozco is a physicist from the Universidad Nacional Autónoma de México (UNAM, Distrito Federal, Mexico). He obtained his Master's degree in physical sciences from UNAM (Distrito Federal, Mexico). He is currently a 2nd-year graduate student in the energy engineering PhD program at IER-UNAM. His research is related to solar chemistry and solar reactor design for solar fuel production. He is also interested in the thermodynamics of vitreous and amorphous states.

Camilo Alberto Arancibia Bulnes

Camilo Alberto Arancibia Bulnes, a physicist from the Benemérita Universidad Autónoma de Puebla (BUAP, Puebla, Mexico), obtained an MSc in optics (INAOE, Puebla, Mexico) and a PhD in physics (CINVESTAV, Merida, Mexico). He has been Senior Researcher at IER-UNAM since 2004. His main research interests are related to optics, radiation and heat transfer in solar concentration systems, with applications to solar chemical reactors and central receiver technology. From 2007 to 2010, he coordinated the team that developed UNAM's 30 kW high radiative flux solar furnace. He is a regular member of the National Academy of Sciences (Mexico) and the National System of Researchers.

Claudio Estrada Gasca

Claudio Estrada Gasca is a physicist from UNAM and has a PhD degree in mechanical engineering from the New Mexico State University, USA. Areas of specific interest are transport phenomena in solar systems, mainly in solar concentration systems. He has been President of Asociación Nacional de Energía Solar and a member of the Board of Directors of International Solar Energy Society. At present, he is a member of the National Council of Renewable Energy (Consejo Consultivo de Energías Renovables) of the Mexican government. He has won several awards, the most recent of which was the award from the Mexican Society of Physics for the Development of Physics in Mexico in 2009. He is one of the most active and important promoters of solar energy in Mexico.